Grinding Performance Integrated Experimental Evaluation on Alumina Ceramics with Leaf-Vein Bionic Grinding Wheel

Chao Li
Jia Duan
Zhang Xiaohong (jansbomb@126.com)
Hunan Institute of Science and Technology, China
Zhaoyao Shi
Guangzhi Yuchi
Songhui Zhang
Wei Li
Dongdong Wen
Shi Luo

Research Article

Keywords: Alumina ceramics, Grinding, Leaf vein, Groove pitch, Wear, Laser ablation

Posted Date: January 14th, 2022

DOI: https://doi.org/10.21203/rs.3.rs-1222982/v1

Abstract

In order to enhance the grinding performance of alumina ceramic materials, the surface of the grinding wheels are ablated by laser radiation before grinding, and the three types of leaf-vein bionic grinding wheels with different micro-groove pitches are formed to compare the grinding experiments with normal grinding wheels. The grinding forces and surface roughness were gauged and the morphological characteristics of ground workpiece surfaces were studied. The results showed that with the increase of groove pitch, the normal grinding force was reduced by 9.6-63%, while the tangential grinding force is reduced by 8.3-42%. The groove can promote the flow of coolant, accelerate the heat dissipation and chip removal in the grinding area, reduce the damage of the workpiece and the wear of the grinding wheel, so the vein bionic grinding wheel had more tremendous processing advantages. Among the four kinds of grinding wheels, the leaf-vein bionic grinding wheel with groove pitch equal to 8mm obtained the best grinding effect. The vein-shaped groove had a positive impact on the grinding process.

1. Introduction

In recent years, a growing number of the alumina ceramics are meeting the challenging needs of wide range of applications such as aerospace, national defence, and other critical industrial areas due to its high hardness, lightweight, chemical corrosion resistance, good wear resistance and heat resistance. However, it is also difficult to process because of its idiosyncratic high hardness and brittleness. How to improve the overall performance of alumina ceramics is the crucial problem of developing core manufacturing technology. Compared with other machining methods, grinding has a profusion of outstanding dominant positions such as high efficiency and high surface quality. Nevertheless, elapsed researchs on the grinding submissions of normal diamond grinding wheels demonstrated that insufficient supply of coolant in the core part of the grinding zone and poor drainage easily induced excessive grinding temperature, thus affecting the grinding quality [1–3].

Texturing grinding wheels as a complementary conditioning step to strengthen the grinding conditions on the surface by producing grooves on the surface of the grinding wheel and thus the overall grinding efficiency had been explored by several researchers. Aurich [4] made a significant improvement in the coolant supply of electroplated cubic boron nitride grinding wheels by milling groove-shaped grooves in the grinding wheel matrix. According to the size of the groove, structured grinding wheels can be divided into micro-structured grinding wheels and macro-structured grinding wheels. Guo et al. [5] studied the effect of a micro-structured surface on the grinding capability of diamond grinding wheels. A significant diminution of the normal forces, the tangential force, the roughness and subsurface damage depth can be implemented in comparison to the polished surfaces. Nonetheless, in the preceding studies, the coolant flow in the working region was inadequate, resulting in severe grinding burns. As a result, it was critical to optimize the cooling conditions. And the studies found that the macrostructure had a better cooling effect. Shi et al. [6] proposed a new spray cooling method used in high-speed grinding. The experimental results exhibite that a structured grinding wheel provides effective cooling with low energy expansion. Zhang et al. [7] found that the grinding temperature of the macro-structured grinding wheel is

32.0% lower than that of the non-structured grinding wheel. Peng et al. [8] studied the effect of a grinding wheel surface with grooves on the cooling efficiency of surface grinding. The results show that the grooved grinding wheel has a higher heat transfer coefficient in the grinding zone compared to the grinding wheel without grooves. And the heat transfer coefficient increases with the number of grooves, so it can be known that the grooves facilitate the accumulation and transportation of the coolant. But, for such systems, it cannot be neglected that due to the irregular arrangement of the grooves, the grinding fluid cannot fully and effectively enter the grinding area during grinding. And the promote in surface roughness and wear rate caused must be discussed.

Studies had shown that the type of geometric structure of the groove had a greater impact on the grinding effect than the structured area [9]. The discontinuous grinding wheel obtained by the surface structuring method of grinding wheel structure design lessened the contact area between the surface of the grinding wheel and the surface of the workpiece in a unit time due to the discontinuity of the surface, and effectively reduced the effects of scratching and ploughing. Therefore, the discontinuous grinding wheel was capable of reducing the grinding force and the grinding damage. In addition, arranging the grinding fluid conveying microporous channel on the grinding wheel surface might further promote the grinding fluid to enter the grinding area, clean the working surface of the grinding wheel, decrease the adhesion of grinding debris, and maintain the sharpness of the cutting edge [10]. As a result, the grinding force and wheel damage were also subsided. Innovative grinding wheel surface structure design realized discontinuous grinding and internal supply of grinding fluid, which was an important method to improve the performance of grinding process.

For decades, to seek a better living environment, plants must transport their nutrients and water to various parts of the body through leaf veins in the fastest way. And finally formed the current leaf vein branch structure. Researchers continue to use this structure. The development and evolution of the company have been applied to different fields for the purpose of obtaining breakthrough progress [11–13]. Zhang et al. [14] introduced the leaf vein bionic theory into the manufacture of the devised grinding wheel. The experimental results showed that the vein structured grinding wheel generated a glossier surface, and the fractal angle had a significant effect on the grinding capability. This also further proved the superiority of the vein structure. However, the grooves on the surface of the grinding wheel would reduce the effective abrasive particles on the surface, and the number of scratches on the workpiece would also be reduced, which would have a negative impact on the surface morphology of the workpiece. Therefore, it was very important to find suitable structured parameters. It has been shown that the pitch of leaf veins also has a considerable impact on the cooling and nutrient transport effects of the leaves [15, 16]. And the structured area of the grinding wheel has an essential influence on the grinding quality [17, 18]. This meat that it was significant to study the effect of the micro-grooves pitch of the leaf-vein bionic grinding wheel on the performance of the grinding wheel.

In the following, several vein structures with different parameters were put forward to cylindrical bronze bond diamond grinding Wheels. The grinding peculiarities of grinding wheels with several different structured parameters were tested and analyzed. Experimental works are comported to investigate the

wheel wear behaviour in grinding with different pitches of micro-grooves by implementing the grinding operations of alumina ceramic on a surface grinder supplied with a bionic grinding wheel with vein structures. The grinding performance was assessed in grinding forces, grinding quality and wear morphology of wheel.

2. Experimental Details

2.1 Laser structuring

The laser ablation method was directly used to remove material from the surface of the workpiece, which could effectively ablate difficult-to-cut materials, and had a high degree of controllability, accuracy and selectivity. It could accomplish a better material removal rate and lower tool wear, while maintaining the surface quality, damage and dimensional accuracy of the processed surface [19–21]. The laser processing technology was also appropriate for brittle and difficult-to-cut materials, and could ensure the process efficiency and material removal rate [22]. In the experiment, a leaf-vein bionic grinding wheel was created utilizing an IPG pulsed fiber laser (model: YCP-1-120-50-50-HC-RG). The average power (P_{avg}) of this laser was 1–50 W, the pulse frequency (f) was 1–200 kHz, the pulse width (τ) was 0.2–25 ms, and the wavelength (λ) was 1064 nm. The Gaussian distribution was used to describe the laser energy output form. A 4-axis laser micro machining workstation was used for the laser processing (X-Y-Z linear, B rotary). To ensure the accuracy and reliability of the experiment, constant laser processing parameters were used to structure the grinding wheel. The grinding wheels were clamped on the rotating shaft of the laser, and the laser beam fell on the upper surface of the grinding wheel to process the grinding wheel. The segmented structuring machining of the grinding wheel was realized by the stepwise rotation of the B axis. In order to obtain a good processing effect, the specific laser processing parameters set were shown in Table 1. The processing times of the macro groove and the micro grooves were a and b, respectively. The leaf-vein bionic processing model was shown in Fig. 1.

Table 1
Laser structuring parameters

Parameter	Spot size d_f [μm]	Average laser power P_{avg} [W]	Pulse frequency f_p [kHz]	Scan speed v_s [mm/s]	Scanning passes N	Focal length f [mm]
macro groove	60	22	25	2200	33	105
micro grooves	60	20	25	1500	28	105

For the sake of exploring the influence of the change of the number of grooves on the processing effect, three kinds of grinding wheels with different structural parameters were processed by laser, and the micro-groove pitch P of each pattern was 6mm, 8mm and 10mm respectively. Other characteristic dimensions of the patterns were the angular orientation of the micro grooves α, the depth and width of

the macro groove were defined as D_1, W_1, D_2 and W_2 were the depth and width of the micro-grooves. The generated patterns and their dimensions were presented in Fig. 2. The groove morphology on the surface of the grinding wheel following laser ablation was depicted in Fig. 3.

2.2 Grinding experiment

The experiment was conducted on the CNC high precision surface grinding machine MGK7120, as shown in Fig. 4. The leaf-vein bionic grinding wheels and normal diamond grinding wheels with different branch vein pitches were used to carry out grinding experiments on alumina ceramics to understand the effect of the number of grooves in the vein structure on the grinding quality. The work material was held by a vice which was secured on a dynamometer (type: Kistler9272) fixed below the workpiece to monitor the normal and tangential forces. The force signal was conducted through the dynamometer, collected by the data acquisition system and noted by the computer. For the ground surface, a 3D measuring laser microscope (OLS5000) was adopted to measure the roughness and observe the damage on the exterior of the workpiece. In addition, the wear of the grinding wheel surface morphology under different pitches of micro-grooves during the grinding process was inspected by a three-dimensional (3D) microscope with an ultralarge depth-of-field (ULDF; type: VHX-5000). During the experiment, a soluble oil solution with a concentration of 5% was used as the coolant. And the specific grinding parameters always remained constant during the processing. Table 2 shows the detailed grinding parameters.

Table 2
Parameters used in grinding of alumina ceramics

Parameter	Value	Parameter	Value
Machine tool	bronze-bond diamond grinding wheel	Wheel surface speed V_s (m/s)	30
Material	Alumina ceramics	Depth of cut a_p (μm)	2, 4, 6, 8
Dimension	25 mm (L) × 25 mm (W) × 7mm (D)	Feed rate v_f (mm/min)	2000
Grinding coolant	Water-based coolant (Type W20)	Micro grooves pitch (mm)	6, 8, 10

3. Results And Discussion

3.1. Effect of pitch of micro grooves on grinding force

The grinding performance was studied under varying pitches of micro-grooves at a constant spindle speed. The influence of different grinding depths on normal (F_n) and tangential (F_t) grinding forces were shown in Fig. 5. The measurement of the grinding force revealed a significant distinction between normal grinding wheels with different microstructure pitches and leaf-vein bionic grinding wheels.

The undeformed chip thickness of workpiece was the most important factor in determining grinding force and surface quality. The following equations (1) can be used to characterize the undeformed chip thickness of a single diamond grain workpiece [2]:

$$h_m = \left[\frac{3}{Ctan\alpha} \left(\frac{v_w}{v_s} \right) \left(\frac{a}{d_e} \right)^{\frac{1}{2}} \right]^{\frac{1}{2}} \quad (1)$$

where h_m is the undeformed chip thickness, C is the abrasive grain density, α is the semi-included grit angle, v_w is the workpiece speed, v_s is the wheel speed, a is the depth of cut and d_e is the equivalent diameter of grinding wheel. When the grinding depth increased, the undeformed chip thickness of the workpiece became thicker, and the grinding force would increase accordingly.

It can be seen from the figure that when the cutting depth was small, the grinding force of different groove spacing had a small difference in grinding force. This might be because it was ductile removal at this time, and the groove had little effect on the grinding force. While the cutting depth increased, the grinding force fluctuated, which might be due to the change in the volume of coolant inside the groove and the thickness of the undeformed chip [23]. As the grinding depth increased, the grinding force had an increasing trend, and the change trend of the normal grinding wheel (P=0) and the leaf-vein bionic grinding wheel was similar. When the grinding depth increased, the maximum undeformed chip thickness was larger than the critical depth of cut for ductile-brittle transition, and the material was removed by brittle fracture [24]. Concurrently, the grinding depth increased, and the grinding contact arc length also enlarged.

At the same grinding depth, compared with normal grinding wheels, the normal grinding force of the vein bionic grinding wheel was effectively reduced by 9.6-63%, and the tangential grinding force is reduced by 8.3-42%. The change of grinding force becomes more and more as the cutting depth increased, which indicates that the way of material removal has gradually changed from plastic removal to brittle fracture and material powder removal.

The grinding force decreased with reducing of the pitch of micro-grooves. The smallest grinding force occurred at the smallest pitch. The reduction in grinding force can not only be attributed to the presence of grooves, which can promote better coolant fluidity and wear debris removal. It is also due to the reduction in the contact area between the grinding wheel and the grinding surface of the workpiece during operation, which leads to a reduction in the number of scratches. And the lower grinding force indicates that the vein bionic grinding wheel with low micro-groove pitch could remove more material from a workpiece before it burned or the tool failed.

For the grinding process, the grinding ratio G was a considerable index to evaluate the wear of the grinding wheel.

$$G = \frac{F_n}{F_t} \quad (2)$$

The normal-to-tangential grinding ratios for alumina ceramic using normal grinding wheel and leaf-vein bionic grinding wheels with different pitches were plotted in Fig. 6. By contrast, grinding wheel with *P*=10mm yielded the minimum *G* value, followed by grinding wheel with *P*=8mm. A larger grinding ratio usually indicates less tool wear, excellent wear resistance and long service life. Although the grinding force in both directions showed a similar downward trend, the normal grinding force reduced quicker than the tangential grinding force, as seen in Fig. 6. The larger the grinding force ratio, the sharper the abrasive grains and the better the performance of the grinding wheel. At the same time, the normal grinding force was lowerer, indicating that the load of the workpiece and the grinding wheel was lesser, so the wear of the grinding wheel was fewer and the workpiece appearance was better. The tangential grinding force was greater, which was conducive to the removal of the material, and the grinding efficiency was higher. Therefore, the comprehensive grinding performance of the two vein bionic grinding wheels with groove spacing of *P*=10 and *P*=8 was better.

3.2. Effect of pitch of micro-grooves on grinding quality

3.2.1 The nature of surface roughness: *Ra* and *Rt*

This part used the results of *Ra* and *Rt* to quantify the surface roughness of the workpiece. Even if two workpieces had the same *Ra* value, a surface with a larger *Rt* value was generally considered to be worse. Therefore, it was necessary to combine two parameter values to evaluate the surface quality.

Figure 7, 8 shows the *Rt*, *Ra* and surface morphology of the workpiece surface after four different grinding wheels. The influence of the variation of the micro-grooves spacing on the surface roughness *Ra* was analyzed and studied. The consequences revealed that when the feed depth was constant, the surface roughness *Ra* was improved when the pitch increases. The surface roughness produced by the wheel with normal grinding wheel (*P*=0mm) was the highest, *Ra* value was 1.26μm, and the wheel with *P*=8mm was the smoothest surface (*Ra*=1.17μm). Simultaneously, the *Rt* values were smaller for grooved grinding than the normal grinding wheel irrespective of groove pitch [25]. From the analysis of the data, it can be known that the surface quality of the workpiece does not completely improve with the increase of the groove pitch. These results showed that the existence of grooves not only reduced the number of abrasive particles on the the grinding wheel surface, but also changed the relative distribution of coolant and chips, which has an essential impact on grinding quality. Due to the edge of the vein fractal structure was a relatively flat vertical section structure, the edge structure can also be used as an additional cutting edge throughout the grinding procedure, thereby further improving the grinding performance of the grinding wheel. And as the grinding depth increased, the over-squeezed abrasive particles were effectively crushed and allowed more abrasive particles in the lower layer to participate in the grinding process.

In three kinds of structured grinding wheels with different micro-groove pitches, when the micro-groove pitch increased from 6mm to 8mm, the grinding quality was improved. This could be due to the reduction of effective abrasive particles when a smaller pitch of micro-grooves was formed on the diamond wheel. In other words, when the pitch increased, the chip thickness becomes relatively larger, as shown in Fig. 9. When the micro groove pitch increased to 10mm, the number of grooves reduced, and the cooling performance of the grinding wheel reduced. Therefore, some burns were inevitably produced, and the roughness increased. The roughness of the unstructured grinding wheel was slightly higher than that of the leaf-vein bionic grinding wheel with P=8mm. This was because the fractal structure of leaf veins had different scales of macroscopic flow channels and microscopic grooves, and the coolant could flow better in the grinding contact area. Thus, we concluded that the effect of the pitch of micro-grooves on the surface roughness was eventful.

3.2.2 Analysis of workpiece surface defects

When the depth of cut was 8μm, the surface morphology of the workpiece produced using different grinding wheels were shown in Fig. 10. Several kinds of defects were usually observed on the surface of the workpiece: cavities, cracks, scratches, furrows, fragments, and material debris. Many scratches and cracks were heeded on the machined surfaces, as shown in Fig. 10(a) - (d). After the grinding experiment, due to the stress and the brittle fracture tendency of the ceramic, cracks would appear in the ceramic and began to grow. Since the groove pitch affected the grinding force, it can be seen that the formation and propagation of cracks were closely related to the grinding force. When the cracks extended to the surface and inside of the material, fragments would be formed. When the fracture propagation within the workpiece ultimately stopped, some residual cracks would form on the surface of workpiece. Furthermore, the number of scratches tended to increase as the micro groove pitch increased. This could be attributed to the fact that during the grinding process, with the shedding and wear of abrasive grains, the increase and accumulation of temperature in the processing area caused graphitization of the surface of the diamond grinding wheel, which affected the surface quality of the workpiece [26]. In addition, the cavities were shown by magnifying the workpiece surface, seeing in Fig. 10(a1) - (d1). This was mostly due to the internal crack propagation during the material removal step and the intergranular breakage of the grinding wheel bond [27].

3.3. Wear morphology of wheel

This part focused on the wear of the wheel by observing the wheel topography. Grinding wheel wear was caused by the counteraction force of the workpiece on the abrasive grains and bonding agent during the grinding, which mainly includes wear flat, grain fracture, and grain pullout. In different stages of the grinding process, the main wear style of the grinding wheel was different. The generated force and moment increased rapidly when the grinding wheel comed into contact with the workpiece. When the stress exceeded the strength of bond, the abrasive particles started to fall off. The greatest force appeared first at the top of the abrasive grains, causing cracks to form, which then extended forward and

expanded downwards, eventually causing the abrasive grains to fracture.During the initial grinding phase, the primary wear style of the grinding wheel was the fracture of the bond. As the grinding wheel gradually stabilizes, it turns into abrasion wear [28].

The wear surface of the grinding wheel under different groove pitches when the grinding depth was 8μm was observed, as shown in Fig. 11. Several different grinding wheels had different wear characteristics under the same grinding conditions. Compared with the the normal grinding wheel surface, the wear mode of the leaf-vein bionic grinding wheel was mainly wear flat, and the phenomenon of abrasive grain fracture and grain pullout was less. It was mainly due to the discontinuous the grinding wheel surface, which facilitated the grinding fluid to enter the grinding zone more acceptable. Only a little amount of coolant could flow into the grinding area without grooves, and the lubricating effect was poor. The groove served as a path for coolant inflow and remain in the channel. The lubricating coating could provide lubrication between the abrasive and the workpiece when the abrasive particles came into touch with it again. So as to achieve adequate lubrication and cooling, lessened the blockage of the grinding wheel surface, and reduced the generation of stress. When each diamond particle was shattered, the vibration between the grinding wheel and the material not only boosted the material removal efficiency of alumina, but it also caused mechanical strain. Simultaneously, the periodic fracture of diamond abrasive grains could form sharp cutting edges to maintain their self-sharpening properties during the grinding process, thereby improving the grinding performance [29].

Nonetheless, in the normal grinding wheel, it was found that the grain pullout and the grain fracture were more serious. This may be due to the small moving space of the grinding fluid and grinding debris in the grinding area, the increased load and the accumulation of grinding heat. As a result, extra predefined breaking points and edges were introduced into the abrasive layer. The number of effective cutting edges decreased as the abrasive granules prolapse. The adhesion layer, which was made up of abrasive debris, diamond debris, and bronze bond debris, enhanced friction between the grinding wheel surface and the working surface, resulting in a high grinding force and heat generation [30, 31]. Because the pressures exerted on the grain were high enough to break the connection, the bond fractures. This resulted in the formation of bulky pits, minor wheel loading, and chip adherence on the wheel surface. Although both the leaf-vein bionic grinding wheel and the normal grinding wheel had minor grain pullouts, the number of grain pullouts in the normal grinding wheel was more significant than that in the leaf-vein bionic grinding wheel. When the downward feed rate per unit time was very low, the grinding heat was transferred to the workpiece at a faster rate than the downward feed rate, which increased the temperature of the grinding process. As a result, the abrasive particles fell off due to the softening of the binder at the front of the grinding wheel. When the downward feed per unit time increased, this softening effect reduced, and the phenomenon of abrasive particle shedding decreased. When the downward feed rate per unit time increased to a certain extent, the volume of the generated wear debris exceeded the chip holding capacity between the abrasive particles, and the force of the abrasive particles increased and fell off. In the grinding process, the effective cutting edges number and cooling effect of the leaf-vein bionic grinding wheel surface were better than that of normal grinding wheels, so the surface appearance of the grinding wheel was better. And the number of abrasive particles per unit area reduced as the abrasive particles fell

off, increasing the thickness of undeformed chips and resulting in poor surface quality of the workpiece [32].

On the surface of these grinding wheels, the fracture of the abrasive grains was also observed. This was because the fragments generated during the grinding of alumina entered the gap between the abrasive grains, and as the grinding progressed, the diamond abrasive grains were repeatedly pressed to cause indentation fatigue, which eventually led to the grinding process. The grains were broken. However, as the groove pitch decreased, the fracture situation improved significantly. Therefore, the fluidity of the coolant caused by different groove pitches had an important influence on the wear of abrasive particles.

4. Conclusions

In this research, pulsed lasers were used to process the surface of diamond grinding wheels to form structured grooves. The laser technique provides for exact control of the produced dimensions of features. To explore the effect of the groove pitch on the grinding effect of the tools, three types of leaf-vein bionic grinding wheels with varied micro groove pitch and normal grinding wheels were used to grind alumina ceramics. Grinding force, workpiece surface morphology, roughness, and grinding wheel surface wear were all measured and compared. The results are summarized as follows:

1. The normal grinding forces of the leaf-vein bionic grinding wheels were reduced by 9.6-63%, while the tangential grinding forces were reduced by 8.3-42%. The fractal pattern improved the fluid flow capacity across the contact region, resulting in an improved ability to capture and eliminate debris from the groove.
2. Compared with normal grinding wheels, the leaf-vein bionic wheel wears less, indicating that the grooves were conducive to the inflow of coolant and reduce the burn of the grinding wheel.
3. The experimental results demonstrated that employing the leaf-vein bionic grinding wheel with groove pitch P=8mm resulted in the best alumina ceramic surface quality, and the surface finish of the workpiece treated by P=10mm was superior than that of P=6mm. Therefore, in the leaf-vein bionic grinding wheel, the best groove pitch was between 8-10mm.

Declarations

Acknowledgements This project was sponsored by the National Key R&D Program of China (grant no. 2018YFB2001400), the National Natural Science Foundation of China (grant no. 51875200), the Natural Science Foundation for Distinguished Young Scholar of Hunan Province (grant no. 2021JJ10031), the National Natural Science Foundation of China Youth Project (grant no. 51905170), the Hunan Provincial Innovation Foundation for Postgraduate (grant no. YCX2021A46). The authors would thank Dr. Dongdong Wen for his experimental support and analysis assistance.

Code availability Not applicable

Data availability All data is available in the manuscript.

Ethics approval Not applicable

Consent to participate Not applicable

Consent for publication Not applicable

Conflict of interest The authors declare no competing interests.

References

1. J. X. Chen, J. B. Qin, L. H. Lu (2019) Study on laser-stricken damage to alumina ceramic layer of different surface roughness. Results in Physics 15, 102723
2. A. Choudhary, A. Naskar, S. Paul (2018) Effect of minimum quantity lubrication on surface integrity in high-speed grinding of sintered alumina using single layer diamond grinding wheel. Ceramics International 44, 17013-17021
3. A. Choudhary, S. Paul (2020) The wear mechanisms of diamond grits in grinding of alumina and yttria-stabilized zirconia under different cooling-lubrication schemes. Wear 454-455
4. J. C. Aurich, B. Kirsch (2013) Improved coolant supply through slotted grinding wheel. CIRP Annals 62, 363-366
5. B. Guo, M. Wu, Q. Zhao, H. Liu, J. Zhang (2018) Improvement of precision grinding performance of CVD diamond wheels by micro-structured surfaces. Ceramics International 44, 17333-17339
6. C. Shi, X. Li, Z. Chen (2014) Design and experimental study of a micro-groove grinding wheel with spray cooling effect. Chinese Journal of Aeronautics 27, 407-412
7. X. Zhang, Z. Zhang, Z. Deng (2019) Precision grinding of silicon nitride ceramic with laser macro-structured diamond wheels. Optics & Laser Technology 109, 418-428
8. R. Peng, J. Tong, X. Tang, X. Huang, K. Liu (2021) Application of a pressurized internal cooling method in grinding inconel 718: Modeling-simulation and testing-validation. International Journal of Mechanical Sciences 189
9. C. Walter, T. Komischke, E. Weingärtner, K. Wegener (2014) Structuring of CBN Grinding Tools by Ultrashort Pulse Laser Ablation. Procedia CIRP 14, 31-36
10. E. Uhlmann, L. Hochschild (2013) Tool optimization for high speed grinding. Production Engineering 7, 185-193
11. A. Bejan, M. R. Errera (2015) Technology evolution, from the constructal law: heat transfer designs. International Journal of Energy Research 39, 919-928
12. T. Miao, A. Chen, L. Zhang, B. Yu (2018) A novel fractal model for permeability of damaged tree-like branching networks. International Journal of Heat and Mass Transfer 127, 278-285

13. P. Xu, A. P. Sasmito, C. Li, S. Qiu (2016) Global and local transport properties of steady and unsteady flow in a symmetrical bronchial tree. International Journal of Heat and Mass Transfer 97, 696-704
14. X. Zhang, Z. Wang, Z. Shi (2020) Improved grinding performance of zirconia ceramic using an innovative biomimetic fractal-branched grinding wheel inspired by leaf vein. Ceramics International 46, 22954-22963
15. M. R. Carins Murphy, G. J. Jordan, T. J. Brodribb (2014) Acclimation to humidity modifies the link between leaf size and the density of veins and stomata. Plant Cell Environ 37, 124-131
16. C. F. Huang, C. P. Yu, Y. H. Wu (2017) Elevated auxin biosynthesis and transport underlie high vein density in C4 leaves. Proc Natl Acad Sci U S A 114, E6884-E6891
17. E. J. Silva, B. Kirsch, A. C. Bottene (2017) Manufacturing of structured surfaces via grinding. Journal of Materials Processing Technology 243, 170-183
18. C. Walter, T. Komischke, F. Kuster, K. Wegener (2014) Laser-structured grinding tools – Generation of prototype patterns and performance evaluation. Journal of Materials Processing Technology 214, 951-961
19. A. K. Dubey, V. Yadava (2008) Laser beam machining—A review. International Journal of Machine Tools and Manufacture 48, 609-628
20. A. Fortunato, G. Guerrini, S. N. Melkote, A. A. G. Bruzzone (2015) A laser assisted hybrid process chain for high removal rate machining of sintered silicon nitride. CIRP Annals 64, 189-192
21. A. Zahedi, T. Tawakoli, B. Azarhoushang, J. Akbari (2014) Picosecond laser treatment of metal-bonded CBN and diamond superabrasive surfaces. The International Journal of Advanced Manufacturing Technology 76, 1479-1491
22. B. Azarhoushang, B. Soltani, A. Zahedi (2017) Laser-assisted grinding of silicon nitride by picosecond laser. The International Journal of Advanced Manufacturing Technology 93, 2517-2529
23. X. Chen, Y. Liang, Z. Sun (2021) Grinding performance oriented experimental evaluation on TiC-Steel cermet with vitrified bond cBN wheel. Ceramics International 47, 34949-34958
24. J. Dai, H. Su, Z. Wang (2021) Damage formation mechanisms of sintered silicon carbide during single-diamond grinding. Ceramics International 47, 28419-28428
25. F. W. Pinto, G. E. Vargas, K. Wegener (2008) Simulation for optimizing grain pattern on Engineered Grinding Tools. CIRP Annals 57, 353-356
26. W. Wang, P. Yao, J. Wang (2016) Crack-free ductile mode grinding of fused silica under controllable dry grinding conditions. International Journal of Machine Tools and Manufacture 109, 126-136
27. Z. Ma, Q. Wang, J. Dong, Z. Wang, T. Yu (2021) Experimental investigation and numerical analysis for machinability of alumina ceramic by laser-assisted grinding. Precision Engineering 72, 798-806
28. Q. Zhang, Q. Zhao, S. To, B. Guo, W. Zhai (2017) Diamond wheel wear mechanism and its impact on the surface generation in parallel diamond grinding of RB-SiC/Si. Diamond and Related Materials 74, 16-23

29. F. Feucht, J. Ketelaer, A. Wolff, M. Mori, M. Fujishima (2014) Latest Machining Technologies of Hard-to-cut Materials by Ultrasonic Machine Tool. Procedia CIRP 14, 148-152
30. Z. Liang, X. Wang, Y. Wu (2012) An investigation on wear mechanism of resin-bonded diamond wheel in Elliptical Ultrasonic Assisted Grinding (EUAG) of monocrystal sapphire. Journal of Materials Processing Technology 212, 868-876
31. Y. Zhang, C. Fang, G. Huang, C. Cui, X. Xu (2019) Numerical and experimental studies on the grinding of cemented carbide with textured monolayer diamond wheels. International Journal of Refractory Metals and Hard Materials 84
32. X. Zhang, Z. Kang, S. Li (2019) Grinding force modelling for ductile-brittle transition in laser macro-micro-structured grinding of zirconia ceramics. Ceramics International 45, 18487-18500

Figures

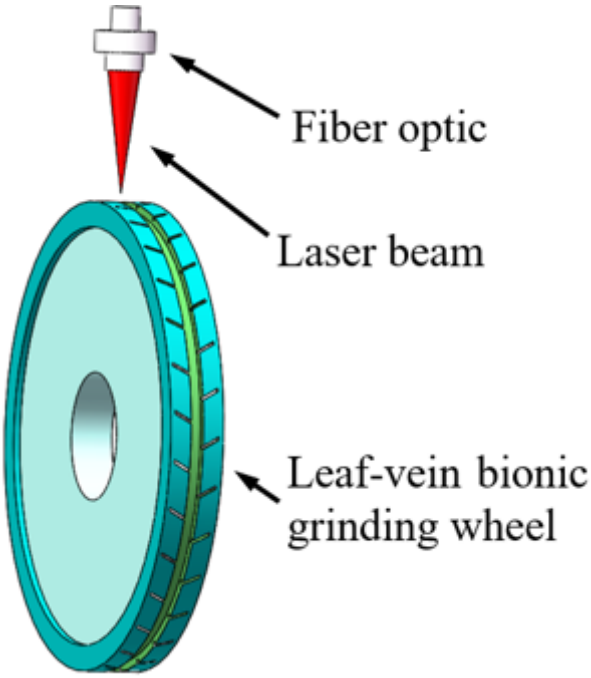

Figure 1

Bionic laser processing model of the veins on the surface of the grinding wheel

Figure 2

The vein pattern on the surface of the grinding wheel and its size parameters

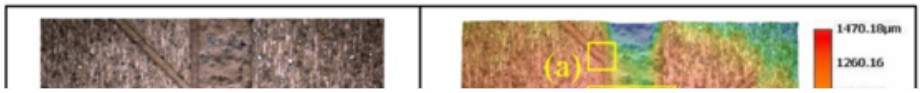

Figure 3

The surface structure of the grinding wheel after processing: (a) the junction of the macro groove and the micro groove, (b) the macro groove, (c) the micro groove

Figure 4

Equipment used in the experiments

Figure 5

Variations of grinding forces during grinding

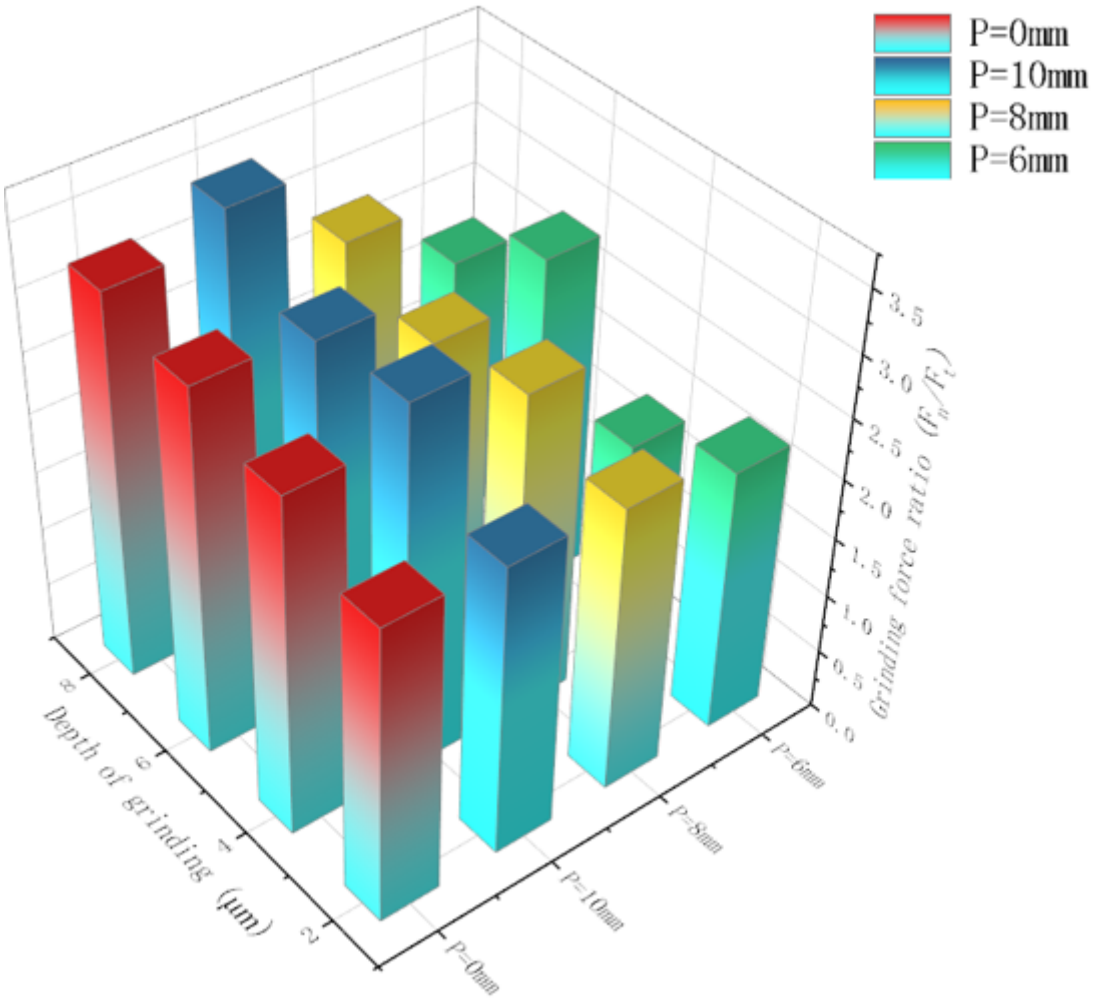

Figure 6

Variations of grinding force ratios during grinding

Figure 7

The surface profile and roughness of the workpiece processed by (a) Normal grinding wheel (b) *P*=6mm (c) *P*=8mm (d) *P*=10mm

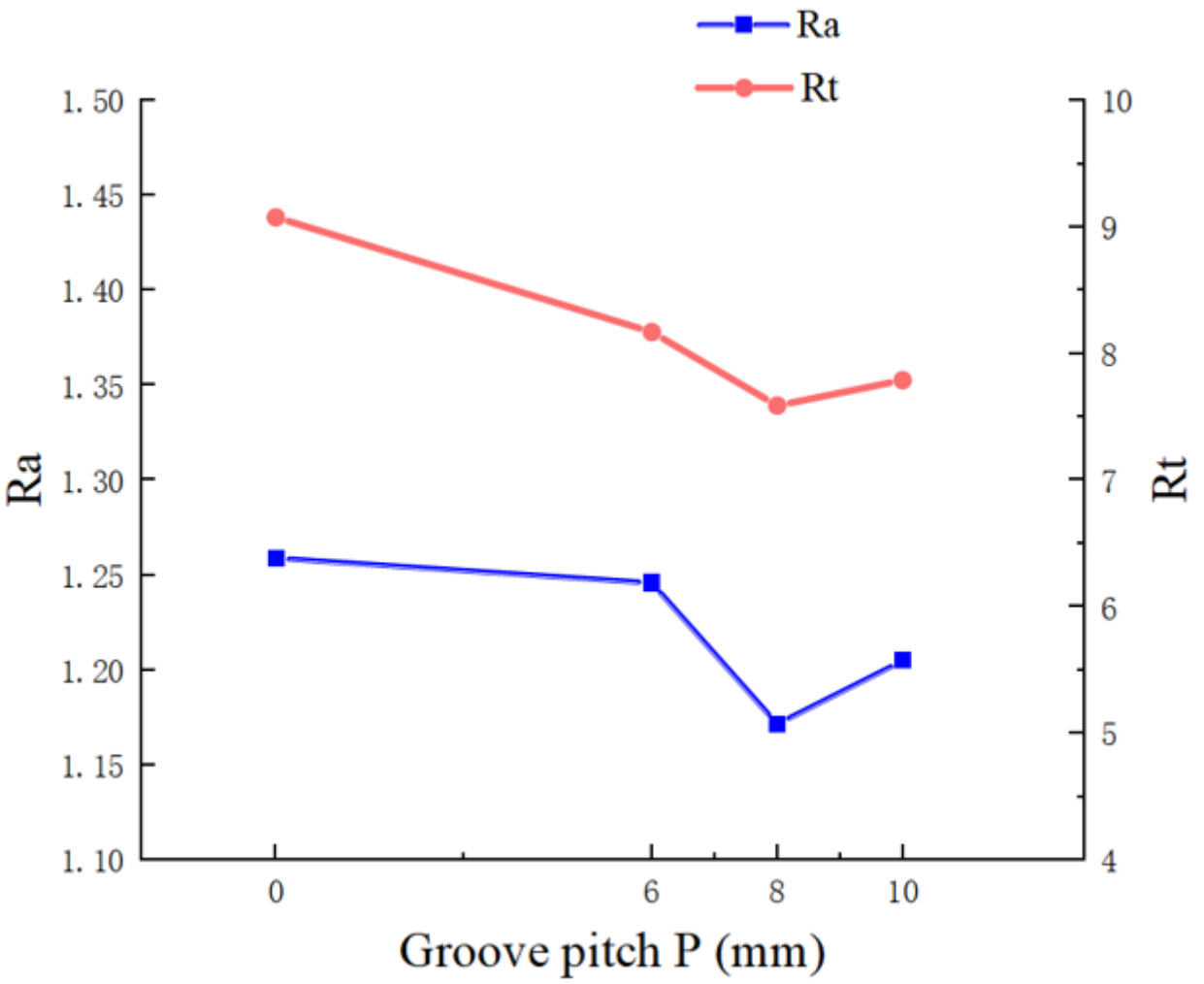

Figure 8

The surface *Ra* and *Rt* of the workpiece processed by the different grinding wheel

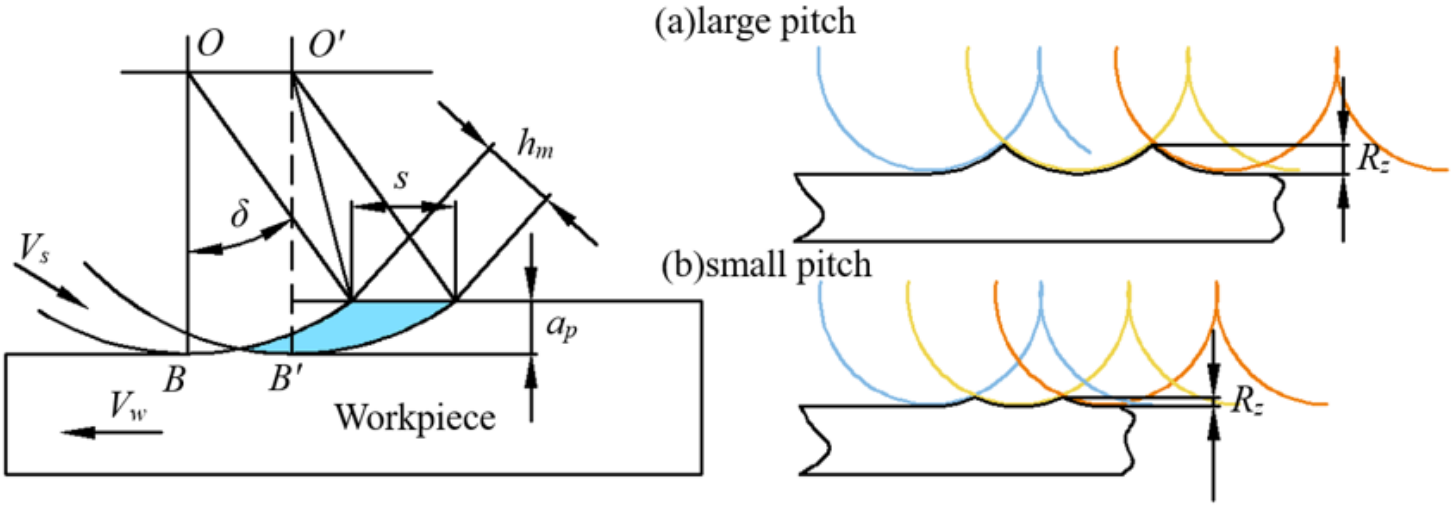

Figure 9

According to the grinding kinematics analysis of the leaf-vein bionic grinding wheel (a) large pitch and (b) small pitch machined maximum undeformed chip thickness

Figure 10

Surface morphology of the workpiece after grinding with (a) Normal grinding wheel (b) *P*=6mm (c) *P*=8mm (d) *P*=10mm

Figure 11

Surface morphology of grinding wheels with different groove pitches after grinding: (a) Normal grinding wheel (b) P=6mm (c) P=8mm (d) P=10mm